Relative Luminosity Analysis for run9 pp 200 GeV Running

James Hays-Wehle, Joe Seele, Hal Spinka, Bernd Surrow

February 6, 2011, Version 0.2

Contents

1 Introduction and Definitions

In any double helicity asymmetry, A_{LL}, measurement there are three important quantities : the polarizations of the two beams, the relative luminosities, and of course the counts of the signal of interest. In this note we detail the calculation of the relative luminosities, various systematic studies, and an estimate of the systematic uncertainty of that quantity. The double helicity asymmetry is written as

$$\begin{aligned} A_{LL} &= \frac{\sigma^{++} + \sigma^{--} - \sigma^{+-} - \sigma^{-+}}{\sigma^{++} + \sigma^{--} + \sigma^{+-} + \sigma^{-+}} \\ &= \frac{\frac{N^{++}}{L^{++}} - \frac{N^{+-}}{L^{+-}}}{\frac{N^{++}}{L^{++}} + \frac{N^{+-}}{L^{+-}}} = \frac{N^{++} - RN^{+-}}{N^{++} + RN^{+-}} \rightarrow \frac{1}{P_B P_Y} \frac{N^{++} - RN^{+-}}{N^{++} + RN^{+-}} \end{aligned}$$

where we have assumed that $\sigma^{++} = \sigma^{--}$ and $\sigma^{+-} = \sigma^{-+}$ and we have defined, the relative luminosity, as $R = \frac{L^{++}}{L^{+-}}$. In order to measure the relative luminosity we need a physics process of interest (or set of them) that we would like to satisfy the following requirements :

1) A high rate, so that the relative luminosity has a smaller statistical uncertainty than our signal of interest.

2) That the reaction be spin independent to a small degree. How well we can guarantee this spin independence will become our dominant systematic uncertainty.

Any uncertainty in the relative luminosity will enter as an uncertainty on the double helicity asymmetry as

$$\delta A_{LL} \simeq \frac{1}{P_B P_Y} \frac{\delta R}{2R} \tag{1}$$

In addition to the one relative luminosity we have defined above, there are a number of other relative luminosities that we can define in order to systematically establish that there is no spin dependence in the rates. The relative luminosities that will be studied in this analysis are defined below.

$$R_1 = \frac{N^{++}+N^{-+}}{N^{+-}+N^{--}} \qquad R_2 = \frac{N^{++}+N^{+-}}{N^{-+}+N^{--}} \qquad R_3 = \frac{N^{++}+N^{--}}{N^{+-}+N^{-+}}$$

$$R_4 = \frac{N^{++}}{N^{--}} \qquad R_5 = \frac{N^{-+}}{N^{--}} \qquad R_6 = \frac{N^{+-}}{N^{--}}$$

$$R_7 = \frac{N^{++}}{N^{+-}} \qquad R_7 = \frac{N^{-+}}{N^{+-}} \qquad R_9 = \frac{N^{++}}{N^{-+}}$$

As you can see from above, the relative luminosity of interest for double helicity asymmetries is defined to be R_3.

One way to check for systematic uncertainties in the relative luminosities is to examine the differences in the different relative luminosities as measured by different high-rate detectors. In this analysis we will use the BBC coincidence rates, the BBC singles rates, the ZDC coincidence rates, and the ZDC singles rates as they should each be sensitive to relatively different physics processes. For example, the difference of the R_3 as measured by the BBC coincidence (BBCX) and the ZDC coincidence (ZDCX) is calculated as,

$$\epsilon(R_3)^{\mathrm{BBCX-ZDCX}} = R_3(\mathrm{BBCX}) - R_3(\mathrm{ZDCX}) \tag{2}$$

The data used to calculate the relative luminosity is the data as recorded in the scaler boards. See appendix blah for an introduction and other relevant information about the scaler boards.

2 Analysis of Raw Data from BBC and ZDC Scalers

This section presents an analysis of the uncorrected (raw) data from the scaler boards. There are a number of boards that STAR uses for scaling purposes. There are two boards that sample both singles counts and coincidence counts from the BBCs and ZDCs, for run 9 they were board 4 and board 6. Board 6 integrated counts throughout an entire DAQ run and board 4 integrated counts over smaller lengths of time ($\sim$5 minutes, but it appears to jump around randomly). There are also two other boards, 11 and 12, that sample the individual inner tiles of the two BBCs, each board sampling a separate BBC.

2.1 Boards 4 and 6 Raw Scaler Counts

In figure **??**, the total raw counts for the 7 interesting possibilities are plotted. The 7 interesting possibilities are the 3 so-called logicals where you have $(\mathrm{X},\mathrm{E},\mathrm{W}) = (1,1,1), (0,1,0)$, and $(0,0,1)$ where X is the coincidence bit for the BBC or ZDC, E is the east bit for the BBC or ZDC and W is the west bit for the BBC or ZDC, and the 4 illogicals where $(\mathrm{X},\mathrm{E},\mathrm{W}) = (1,0,0), (1,1,0), (1,0,1)$ and $(0,1,1)$. If everything was timed in properly and everything was set consistently in the timing windows, there should be no illogicals, but because of timing cuts and timing difference cuts, there are expected to be some physical illiogicals and because of bad timing of signals into boards there are expected to be some unphysical illogicals. The physical logicals can be seen in the BBC $(0,1,1)$ bit configuration for board 4 and a number of unphysical illogicals can be seen in board 6.

Another feature of the raw counts that is not completely understood at the moment is the pattern of relative rates between the singles and coincidences for the BBC and ZDC. For the ZDC the singles rates are much larger than the coincidence rate whereas for the BBC, the opposite is true. At some point as the rate increases beyond a threshold, you expect this to be true, but for average rates of 10% that the BBC saw it isn't expected that this will occur yet, so it likely that the physical mechanism that causes

the BBC hits prefers the case where you get hits in both BBCs as opposed to just one BBC (though this isn't likely to hold for the pp500 running)

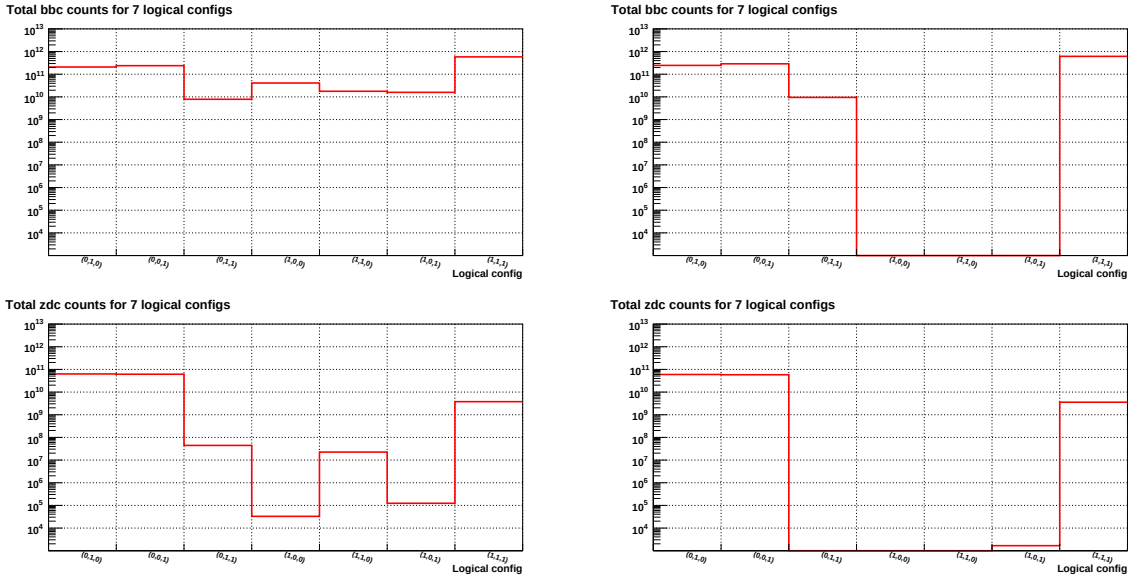

Figure 1: The raw counts from 6 (left) and board 4 (right) for the BBC and ZDC. Both the logicals and illogicals are included to show that board 6 was not timed in very well for the run9 pp200 data taking period, though board 4 appears to be behavior as is expected from the input algorithms.

2.2 Bunch Crossing Number Structure

Additionally, we looked at the structure of these 7 scaler bit possibilities versus bunch crossing number to see if there is any structure that couldn't be explained and there are a number of structures in the data that are not fully understood at the writing of this note. Looking at figure **??**, which is a plot of the BBC rates for the 7 possible configurations of (X, E, W) versus bunch crossing number, you see that there are a number of anomalies in the data. There is a strong rise in the rate after each of the abort gaps. The current hypothesis is that this is due to after-pulsing in some of the PMTs for the BBC inner tiles, but this needs to be studied further before this is confirmed. There is also a large peak in the rate around bunch crossing 80 (specifically bunch crossings 78, 79, and 80). In some of the bit configurations there is also the hint of a "shark's fin" like increase in the rate (after the first abort gap) and this is not currently understand. A similar plot for the ZDC rates can be seen in figure **??** where many of the same artifacts exist implying that they are real artifacts of the bunches in the accelerator and not an artifact of some detector inefficiency or problem.

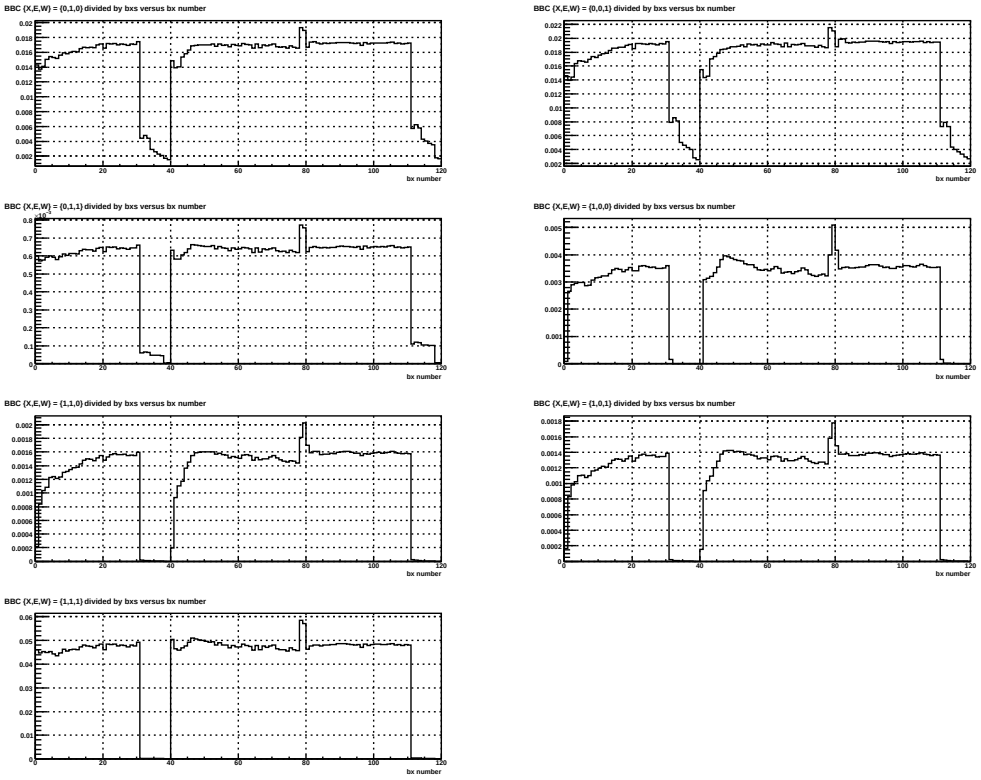

Figure 2: BBC rates for the 7 possibilities versus bunch crossing number

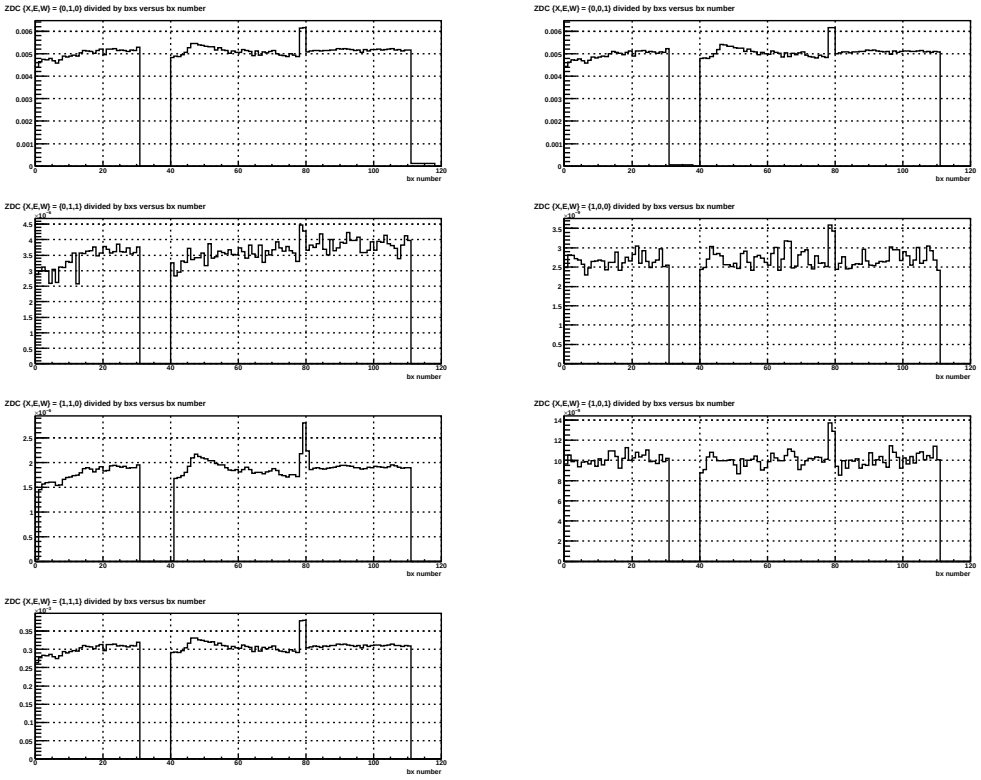

Figure 3: ZDC rates for the 7 possibilities versus bunch crossing number

For spin measurements, the rate effects, the peak around 80 and the "shark's fin" after the first abort gap, are not problems unless they affect the BBC and ZDC differently as this will cause an improper estimate of the relative luminosity or its systematic uncertainty. If we take a ratio of the raw ZDCX to the raw BBCX ($(\mathrm{X}, \mathrm{E}, \mathrm{W}) = (1, 1, 1)$) this will shed light on any of the differences that we need to worry about for this analysis. This quantity is plotted in figure **??**. You can see in the figure that there is a strong difference in the two rates for the artifact near bunch crossing 80, though the shark's fin mostly disappears from notice. And after the rate dependent luminosity corrections are applied, the shark's fin effect (see section 6.blah) will be even less significant, though the artifact near 80 will not become less significant.

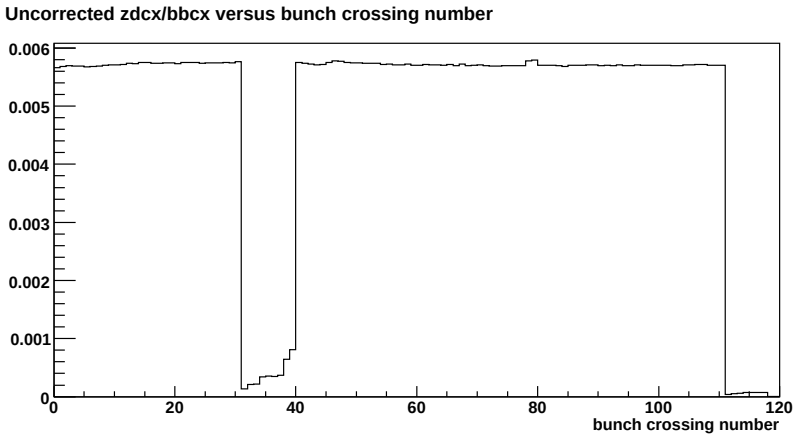

Figure 4: Uncorrected ZDCX/BBCX rates versus bunch crossing number.

2.3 Boards 11 and 12 Raw Scaler Counts

The two BBC inner tiles integrating boards are boards 11 and 12. Their exact mapping from channel to scaler bit can be see in appendix blah. In each scaler board only 16 of the 24 bits were used for scaling and as their are 18 inner tiles (each with its own PMT), two sets of two tubes are joined, and scaled as a single bit. The other 8 bits are dedicated to a vt201 bbcx coincidence bit and 7 bunch crossing bits to give the bunch crossing number. The physical locations of the 16 inputs to scaler boards 11 and 12 can be see in figure **??**.

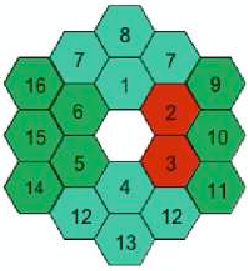

Figure 5: Tube count layout for boards 11 and 12.

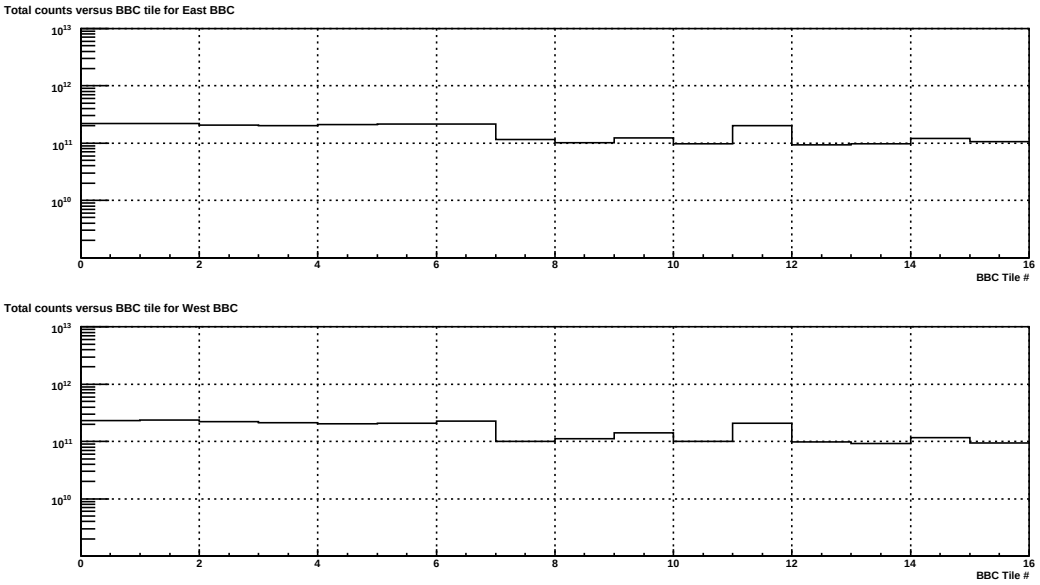

Figure 6: Counts versus tile number for boards 11 and 12. The mapping is the same as in figure **??**

3 Accidentals and Multiples Corrections

There are two types of corrections that must be applied to the scaler data in order to get rates that truly follow the delivered luminosity in a linear fashion. They are called the accidentals and multiples corrections. Accidentals correct for the case where two collision occur in a single bunch crossing that produce hits in opposite BBCs or ZDCs and appear to have been caused by a single collision that caused a coincidence as can be seen in figure blah (TBA).

Similarly multiples corrections account for the case where you have more than one collision that produces hits in a single detector. For example two collisions in a single bunch crossing that both provide hits in both ZDCs as is shown in figure blah (TBA). And as our scaler system cannot distinguish this event from a single collision causing a hit in the ZDC, this leads to an undercounting in the true coincidences.

Because our bunch crossings are not equal in their rates, the corrections are done on a bunch crossing by bunch crossing basis in each scaler board sample.

3.1 Accidentals Corrections

In accidentals corrections we seek to transform our measured singles and coincidence rates into something that is physical and such that multiples corrections can be applied to them. Let us define the following physical quantities, which are not the scaled quantities, but are combinations of them :

- P_A : The probability for the physical processes that provide at least one hit in the east detector and no where else (i.e. not a coincidence)
- P_B : The probability for the physical processes that provide at least one hit in the west detector and no where else.

- P_C : The probability for the physical processes that cause at least one coincidence hit in the east and west detectors and are not two single processes causing a hit in the two detectors.

It is these physical processes that we would like to use to calculate our luminosity and relative luminosity as these can be corrected for multiple interactions because they obey Poisson statistics as independent and distinct physical processes. With the physical quantities now defined we can write out the probabilities for the scaled quantities in terms of the probabilities for the physical processes and they are

$$\begin{aligned} P_E &= P_A + P_C - P_A P_C & (3)\\ P_W &= P_B + P_C - P_B P_C & (4)\\ P_{EW} &= P_C + P_A P_B - P_C P_A P_B. & (5) \end{aligned}$$

We can then invert these equations to find the physical probabilities in terms of the scaled probabilities which are

$$\begin{aligned} P_A &= \frac{P_E - P_{EW}}{1 - P_W} & (6)\\ P_B &= \frac{P_W - P_{EW}}{1 - P_E} & (7)\\ P_C &= \frac{P_{EW} - P_E P_W}{1 + P_{EW} - P_E - P_W}. & (8) \end{aligned}$$

3.2 Multiples Corrections

When we scale quantities what we actually measure is not the actual number of processes that occur, which is what scales with luminosity, but the number of bunch crossings where at least 1 physical process occurred. The distribution of how many physical processes occur in a bunch crossing is described by the Poisson series,

$$P(\lambda) = \sum_k \frac{e^{-\lambda}\lambda^k}{k!} \quad (9)$$

where λ is the rate of events in a single bunch crossing and each term in the series, $\frac{e^{-\lambda}\lambda^k}{k!}$ is the probability for k events to occur in a given amount of time (which for us is a single bunch crossing). The rate, λ, is not the probability for a single event to occur in a single bunch crossing, but is the true event rate which we don't measure, but if we can extract this quantity and multiply it by the number of bunch crossings we will have a correct estimate of the true number of physical events that occurred and this is a quantity that will scale linearly with luminosity.

To get λ we will take a round about approach. We first point out that the probability for no event to occur in a bunch crossing is

$$P(\lambda, k = 0) = P_0 = e^{-\lambda} = 1 - P_{\text{something}} \quad (10)$$

where $P_{\text{something}}$ is the probability for something occur in a bunch crossing (i.e. 1 physical event in a bunch crossing, 2 physical events in a bunch crossing, etc) which is exactly our accidentals correct physical scaled quantities, P_A, P_B, and P_C. So inverting this equation we now get

$$\lambda = -\ln\left(1 - P_{\text{something}}\right) \tag{11}$$

and then we can calculate our corrected number of events as

$$N^{\text{scaler}}_{\text{corrected}} = \lambda N_{\text{BX}} \tag{12}$$

where $N^{\text{scaler}}_{\text{corrected}}$ is the true number of physical events that occurred and N_{BX} is the number of bunch crossings. Finally, writing out the final formulas for the corrections in their full glory we arrive at

$$N_A = -N_{BX} \ln\left(1 - \frac{N_E - N_{EW}}{N_{BX} - N_W}\right) \tag{13}$$

$$N_B = -N_{BX} \ln\left(1 - \frac{N_W - N_{EW}}{N_{BX} - N_E}\right) \tag{14}$$

$$N_C = -N_{BX} \ln\left(1 - \frac{N_{EW} - N_E N_W / N_{BX}}{N_{BX} + N_{EW} - N_E - N_W}\right) \tag{15}$$

where $N_{\{E,W,EW\}} = P_{\{E,W,EW\}} N_{BX}$.

3.3 A/M Corrections at STAR

Because STAR uses different definitions for the various singles and coincidence bits, the different scaler bits that were defined in section blah need to be combined together in the appropriate way in order get quantities for which the accidentals and multiples corrections will work properly. In this section we will outline the various approaches that will be tested in later sections. The quantitative evaluation of how well the approaches succeed will be left to later sections in this note, but some qualitative statements about their agreement will be made in the following subsections.

3.3.1 Naive Approach

In this approached we define the E, W and EW quantities, where we again used the (X, E, W) notation,

- E = $(0, 1, 0) + (1, 1, 1)$
- W = $(0, 0, 1) + (1, 1, 1)$
- EW = $(1, 1, 1)$

This approach would be appropriate if there were no TAC difference required for the coincidence trigger which is the case for the ZDC, but as there is for the BBC, this will not be the appropriate definition for the STAR scalers as they were set up in the run9 pp200 running.

3.3.2 Global Approach

Another approach, which is more ad hoc, and can be viewed as being the opposite of the Naive approach, just includes anything that you think could cause a true physical events to occur. This approach is defined as

- E = $(0, 1, 0) + (0, 1, 1) + (1, 0, 0) + (1, 0, 1) + (1, 1, 0) + (1, 1, 1)$

- W = $(0,0,1)+(0,1,1)+(1,0,0)+(1,0,1)+(1,1,0)+(1,1,1)$
- EW = $(1,0,0)+(1,0,1)+(1,1,0)+(1,1,1)$

For the board 6 scalers in STAR, this approach seems to work the best. This is not presently understood.

3.3.3 Super Global Approach

This is the same as the Global approach except that

- EW = $(0,1,1)+(1,0,0)+(1,0,1)+(1,1,0)+(1,1,1)$

3.3.4 TAC Diff Approach

The last approach that will be explored in this note is called the TAC diff approach and this is what the expected setup should be the BBC scalers if everything had been timed in appropriately and there were no sources of beam related background, which is not strictly true because this is why the TAC Diff was applied in the first place. The scaler configurations are defined to be

- E = $(0,1,0)+(0,1,1)+(1,1,1)$
- W = $(0,0,1)+(0,1,1)+(1,1,1)$
- EW = $(0,1,1)+(1,1,1)$

3.4 Inadequacy of Formulas Used

There are a number of effects that are not currently captured by the formulas that are applied for the accidentals and multiples. The formulas assume that the rate at which events can occur is constant, and as our luminosity decreases exponentially throughout the course of a run or fill, this is certainly not true. No substantive studies have been done to estimate how big of an effect this is, though evidence from the agreement of the BBCX and ZDCX as a function of luminosity gives supporting evidence that these corrections are not large at the moment, though they will likely be more important in the 500 GeV running.

4 Agreement Between BBC and ZDC

The section details the comparison of the relative luminosities as seen by the BBCs and ZDCs and as board 6 is the one that will be used for the actual calculation of the relative luminosity (with board 4 providing a good cross check), this rest of this section will only discuss data from board 6. With the BBCs and ZDCs there are 4 independent detectors that are combined into singles and coincidences. All the data that will be examined in this section is calculated using the global approach to the summing for the A/M corrections.

4.1 Relative Luminosity Differences Data

One way to investigate the relative luminosity calculations is to plot the differences of the relative luminosities, ϵ, as measured by two different detectors as a function of runnumber and look for differences from 0 in these quantities. We consider 6 "detectors" at STAR for this study: the BBCE, BBCW, BBCX, ZDCE, ZDCW, and the ZDCX which are the accidentals and multiples corrected physical versions of the raw scalers as defined earlier. That is to say none of them are separate detectors subsystems but are convolutions of the three raw signals : east, west and coincidence. The timeseries data for the relative luminosity differences for 7 different detector combinations are shown in figure **??** through **??**. The means and RMS values of each of the timeseries are documented in tables **??**, **??** and **??**.

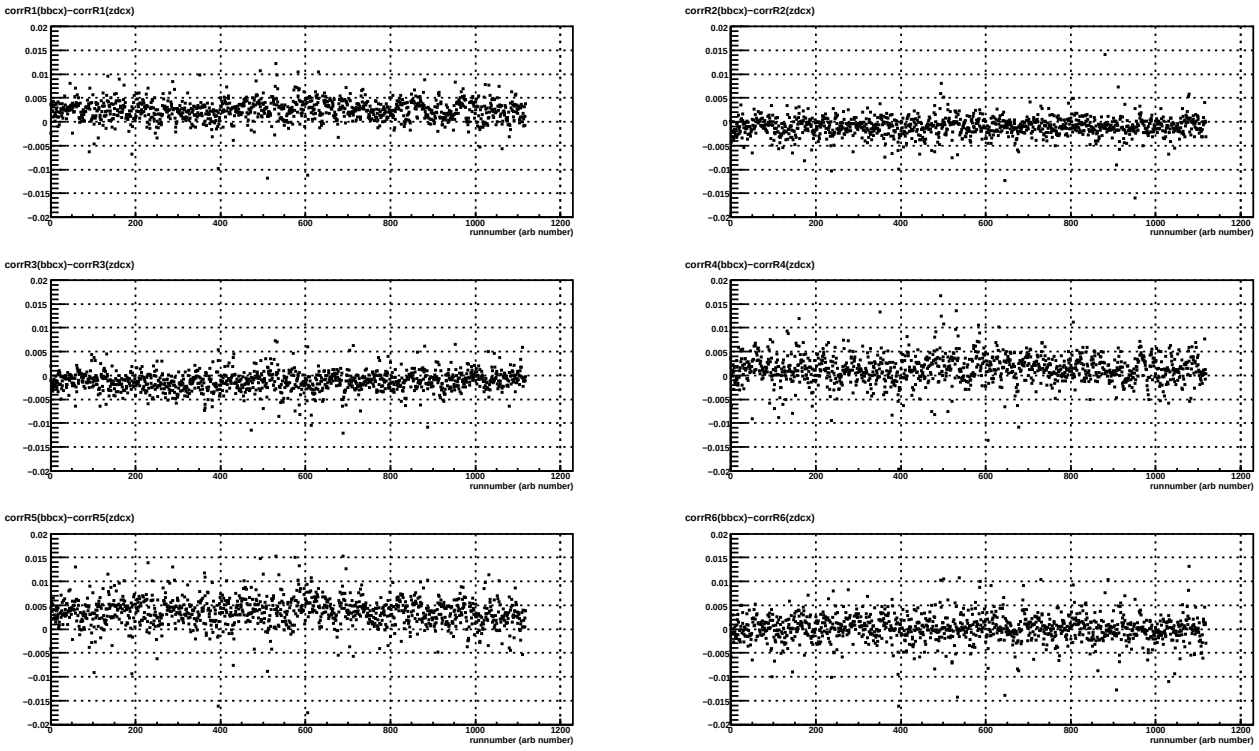

Figure 7: The 6 $\epsilon(R_i)$s for the BBCX-ZDCX versus runnumber (arb. count).

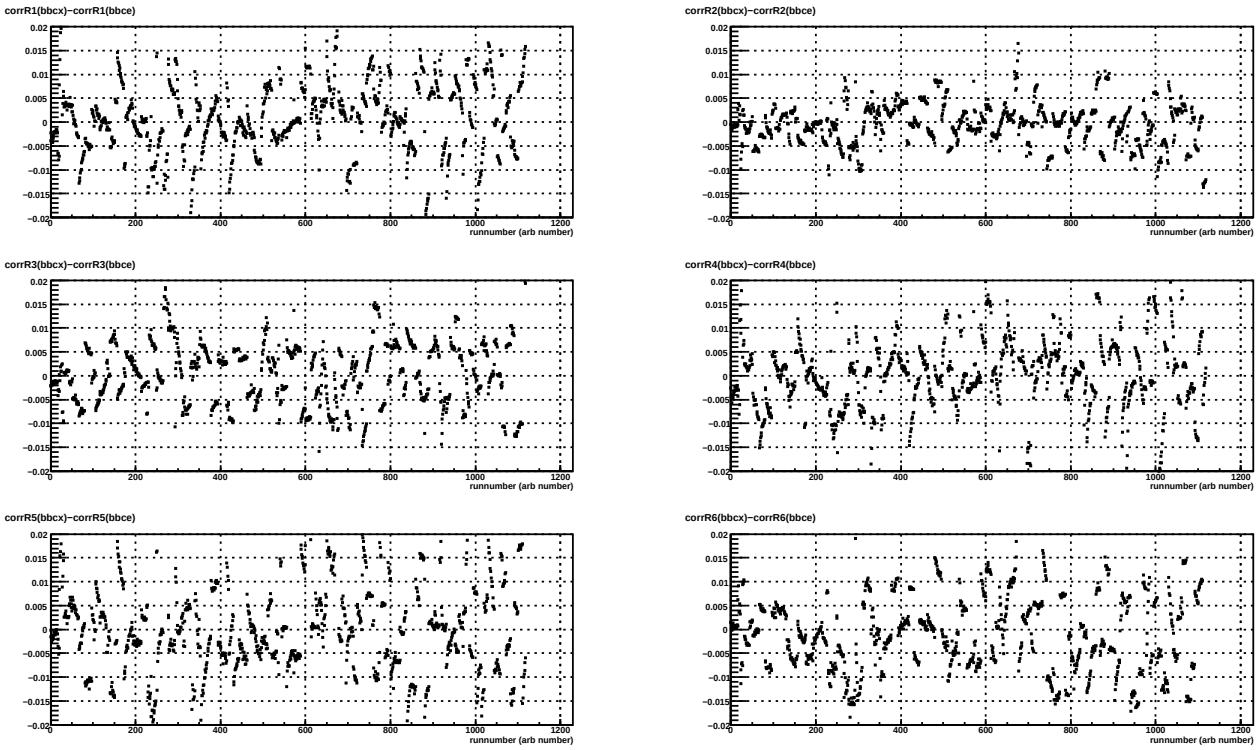

Figure 8: The 6 $\epsilon(R_i)$s for the BBCX-BBCE versus runnumber (arb. count).

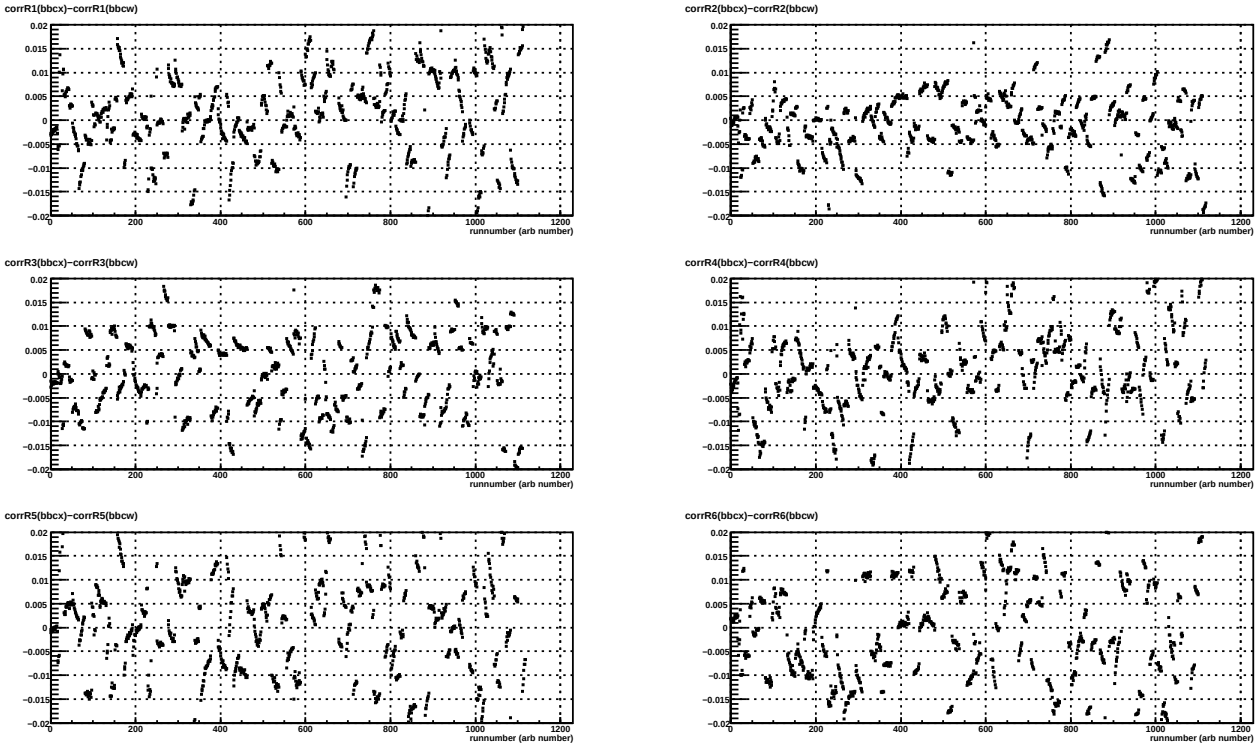

Figure 9: The 6 $\epsilon(R_i)$s for the BBCX-BBCW versus runnumber (arb. count).

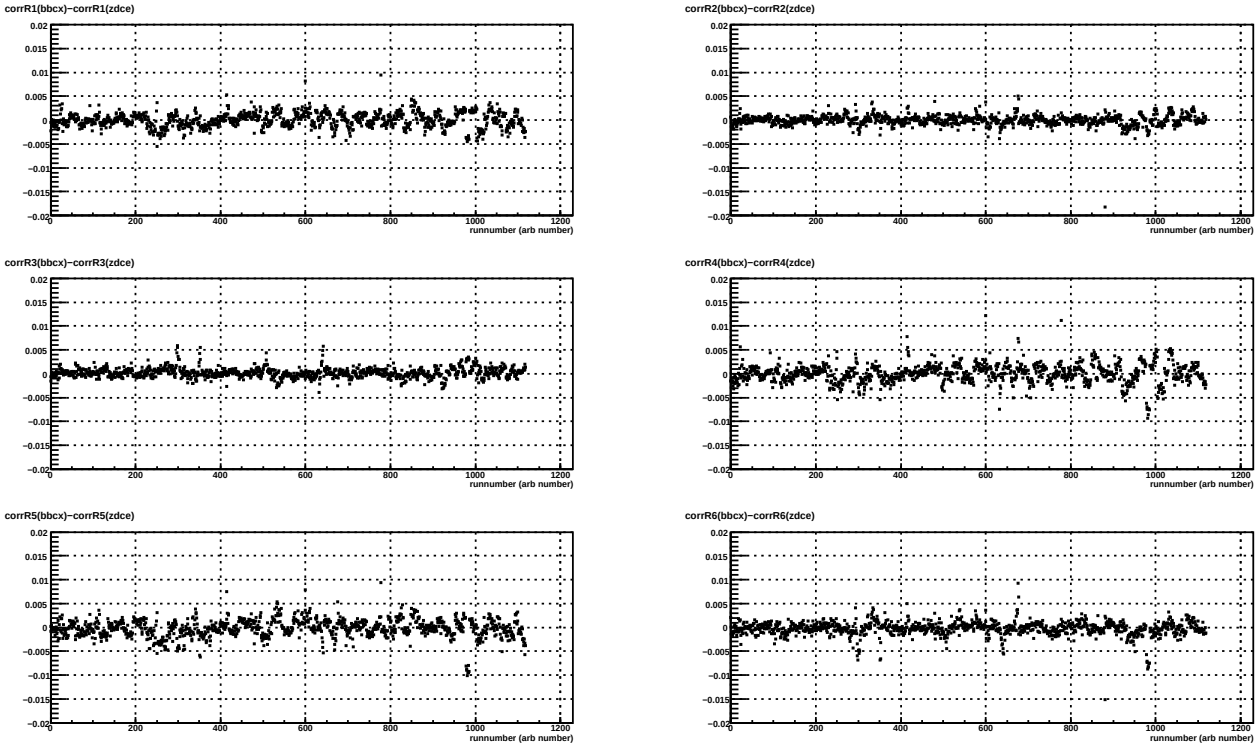

Figure 10: The 6 $\epsilon(R_i)$s for the BBCX-ZDCE versus runnumber (arb. count).

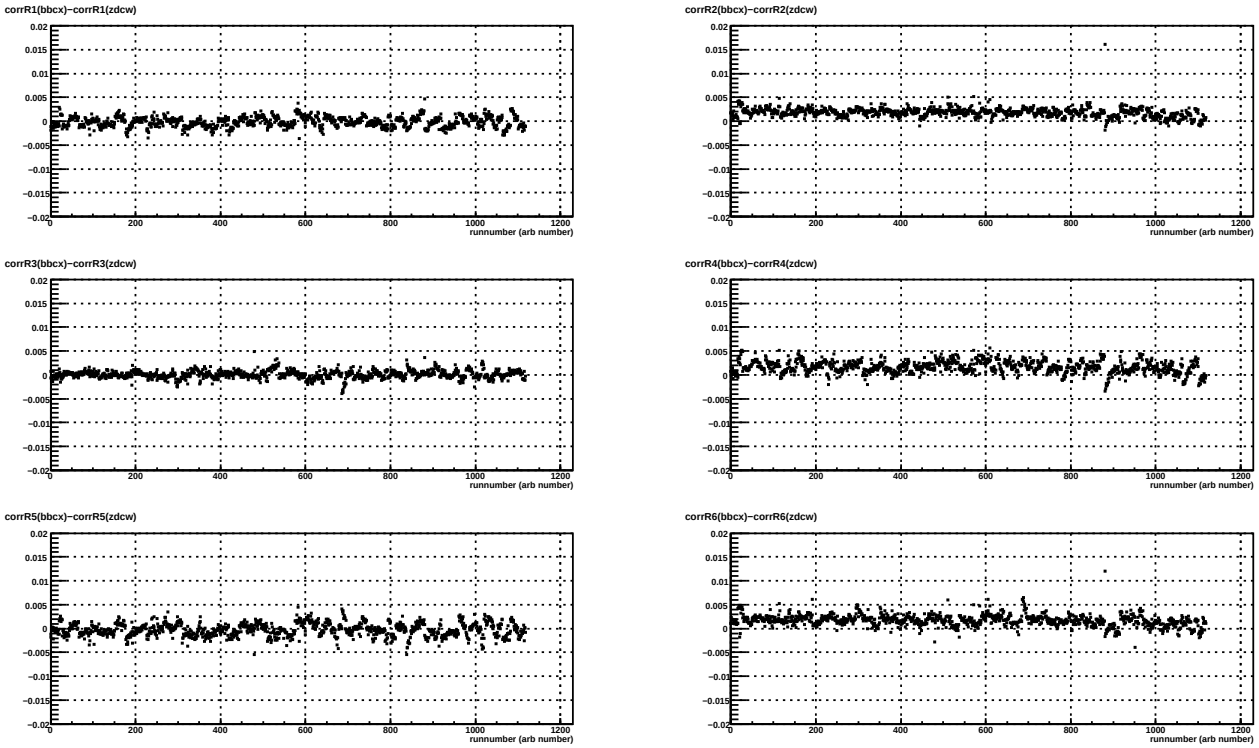

Figure 11: The 6 $\epsilon(R_i)$s for the BBCX-ZDCW versus runnumber (arb. count).

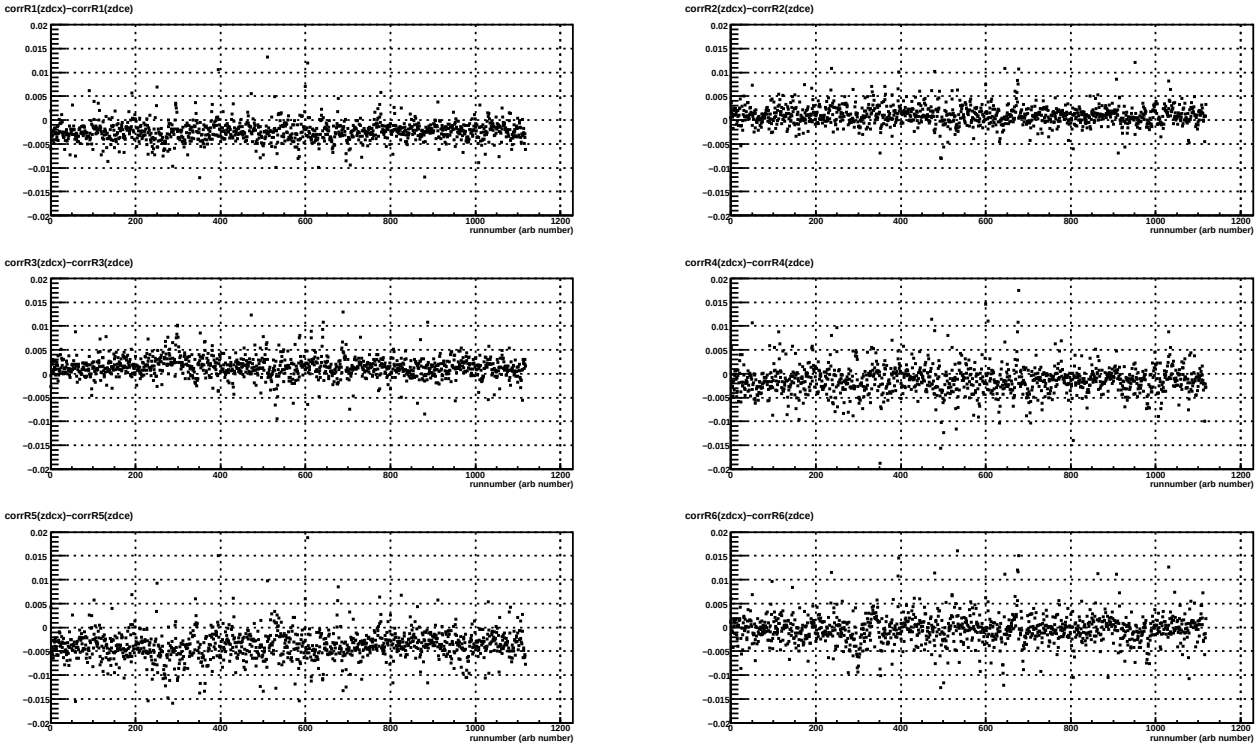

Figure 12: The 6 $\epsilon(R_i)$s for the ZDCX-ZDCE versus runnumber (arb. count).

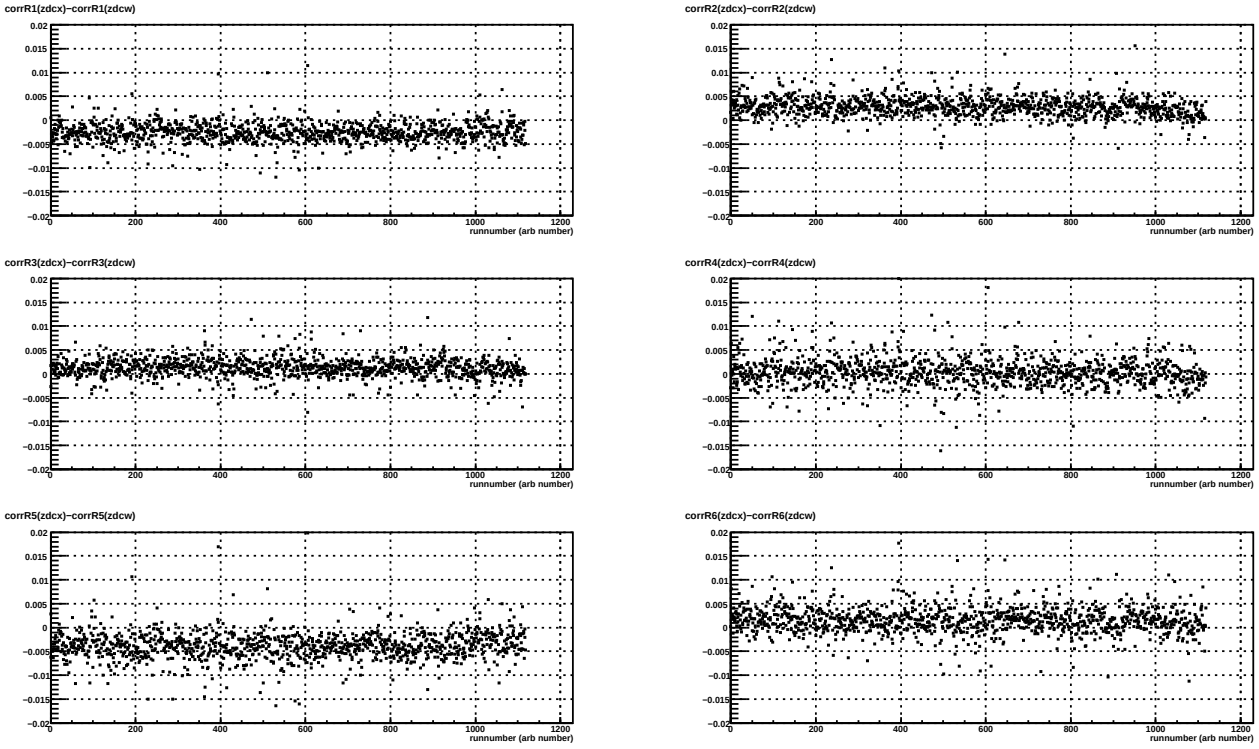

Figure 13: The 6 $\epsilon(R_i)$s for the ZDCX-ZDCW versus runnumber (arb. count).

	BBCX-ZDCX	BBCX-BBCE	BBCX-BBCW
$\epsilon(R_1)$	0.0024 ± 0.0022	0.0009 ± 0.0073	0.0018 ± 0.0090
$\epsilon(R_2)$	-0.0010 ± 0.0020	-0.0004 ± 0.0043	-0.0011 ± 0.0060
$\epsilon(R_3)$	-0.0012 ± 0.0021	0.0005 ± 0.0064	0.0003 ± 0.0083
$\epsilon(R_4)$	0.0014 ± 0.0030	0.0004 ± 0.0082	0.0008 ± 0.0098
$\epsilon(R_5)$	0.0036 ± 0.0030	0.0001 ± 0.0096	0.0012 ± 0.0125
$\epsilon(R_6)$	0.0001 ± 0.0030	-0.0012 ± 0.0085	-0.0017 ± 0.0111
$\epsilon(R_7)$	0.0012 ± 0.0030	0.0014 ± 0.0104	0.0019 ± 0.0122
$\epsilon(R_8)$	0.0034 ± 0.0029	0.0014 ± 0.0091	0.0028 ± 0.0120
$\epsilon(R_9)$	-0.0022 ± 0.0028	0.0000 ± 0.0073	-0.0009 ± 0.0097

Table 1: The relative luminosity differences for the BBCX-ZDCX, BBCX-BBCE and BBCX-BBCW.

	BBCX-ZDCE	BBCX-ZDCW
$\epsilon(R_1)$	0.0000 ± 0.0016	-0.0001 ± 0.0011
$\epsilon(R_2)$	-0.0000 ± 0.0012	0.0018 ± 0.0009
$\epsilon(R_3)$	0.0002 ± 0.0011	0.0001 ± 0.0008
$\epsilon(R_4)$	0.0000 ± 0.0022	0.0017 ± 0.0014
$\epsilon(R_5)$	-0.0002 ± 0.0020	-0.0003 ± 0.0014
$\epsilon(R_6)$	-0.0002 ± 0.0016	0.0017 ± 0.0012
$\epsilon(R_7)$	0.0002 ± 0.0020	-0.0001 ± 0.0014
$\epsilon(R_8)$	0.0001 ± 0.0019	-0.0020 ± 0.0015
$\epsilon(R_9)$	0.0002 ± 0.0017	0.0019 ± 0.0013

Table 2: The relative luminosity differences for the BCCX-ZDCE and BCCX-ZDCW.

	ZDCX-ZDCE	ZDCX-ZDCW
$\epsilon(R_1)$	-0.0024 ± 0.0022	-0.0025 ± 0.0021
$\epsilon(R_2)$	0.0010 ± 0.0023	0.0028 ± 0.0020
$\epsilon(R_3)$	0.0014 ± 0.0023	0.0013 ± 0.0020
$\epsilon(R_4)$	-0.0014 ± 0.0034	0.0003 ± 0.0029
$\epsilon(R_5)$	-0.0038 ± 0.0032	-0.0038 ± 0.0029
$\epsilon(R_6)$	-0.0004 ± 0.0032	0.0016 ± 0.0029
$\epsilon(R_7)$	-0.0009 ± 0.0032	-0.0013 ± 0.0028
$\epsilon(R_8)$	-0.0034 ± 0.0030	-0.0054 ± 0.0028
$\epsilon(R_9)$	0.0024 ± 0.0033	0.0041 ± 0.0028

Table 3: The relative luminosity differences for the ZDCX-ZDCE and ZDCX-ZDCW.

4.2 Relative Luminosity Differences Discussion

There are a number of effects in the last section's data that will be discussed in this section.

BBCX-ZDCX : This relative luminosity difference has been used in the past to estimate the systematic uncertainty in our data sets. There are clear offsets from 0 that persist throughout the entire run regardless of spin pattern and magnetic field configuration. They do not as present correspond to any clear pattern of spin asymmetry effects. Possibilities for the pattern of offsets is discussed in section blah. With this data alone one cannot tell if it is the BBCX that has spin effects, the ZDCX that has spin effects or both. With the other relative luminosity differences it becomes possible to disentangle these hypotheses and we will find that it is the ZDCX that has the large spin effects and not the BBCX.

BBCX-BBCE and BBCX-BBCW : As you can see by looking at the data, there is clearly a systematic problem. The problem is currently though to be a noisy tube in the east BBC (#16). The pattern is still not understood and it has not been investigated anymore at the time of the writing of this note.

BBCX-ZDCE : This data appears to have no sizable systematic offsets from 0 in any of the the quantities to a level of $< 2e-4$. There is noise in the data and it is expected to be from the BBCX (because of the noisy tube) Because these two detectors measure very different physical processes that are sensitive to different spin asymmetries, the fact that they agree to such a level is strong evidence for both of their scales quantities being spin independent to a level $< 2e-4$.

BBCX-ZDCW : This data shows a clear offset from 0 as well, but this data is perfectly consistent with a single spin asymmetry in the blue beam which implies that something correlated with the transverse spin component of the beam. There was a spin rotator tune done late in run9 where the transverse component was decreased in magnitude and this corresponds to a decreased in this offset from 0 lending further evidence to the idea that it is related to a transverse single spin asymmetry (see section blah for more discussion of this correlation).

ZDCX-ZDCE and ZDCX-ZDCW : Here you again see a clear spin pattern dependence and you see that for the ZDCX-ZDCE, the magnitude of the offset is equal and opposite in sign to the BBCX-ZDCX, thus it is consistent with the idea that the ZDCX is the scaled quantity that has spin dependence to it. The ZDCX-ZDCW is consistent with the other observed spin pattern offsets, but it doesn't supply any new information about the cause of the spin pattern dependence.

5 Cross Ratios From Boards 11 and 12

There are a number of quantities that can be calculated using boards 11 and 12. There are quantities that are sensitive to polarization observables in a single beam. Each of the quantities is calculated separately for the east and west BBC. The ones we are interested in are

$$\widetilde{A}^{B}_{N,LR} = \sqrt{\frac{(N_L^{++}+N_L^{+-})(N_R^{-+}+N_R^{--})}{(N_L^{-+}+N_L^{--})(N_R^{++}+N_R^{+-})}} \tag{16}$$

$$\widetilde{A}^{Y}_{N,LR} = \sqrt{\frac{(N_L^{++}+N_L^{-+})(N_R^{+-}+N_R^{--})}{(N_L^{+-}+N_L^{--})(N_R^{++}+N_R^{-+})}} \tag{17}$$

$$\widetilde{A}^{B}_{N,TB} = \sqrt{\frac{(N_T^{++}+N_T^{+-})(N_B^{-+}+N_B^{--})}{(N_T^{-+}+N_T^{--})(N_B^{++}+N_B^{+-})}} \tag{18}$$

$$\widetilde{A}^{Y}_{N,TB} = \sqrt{\frac{(N_T^{++}+N_T^{-+})(N_B^{+-}+N_B^{--})}{(N_T^{+-}+N_T^{--})(N_B^{++}+N_B^{-+})}} \tag{19}$$

Where L, R, T and B are defined as clusters of tubes in each of the BBCs. Their exact definitions in terms of the setup in figure blah is

- L = $\{5, 6, 14, 15, 16\}$ (16 in the east is excluded because it is noisy)
- R = $\{2, 3, 9, 10, 11\}$
- T = $\{1, 7, 8\}$
- B = $\{4, 12, 13\}$

All the counts used were also required to satisfy the vt201 bit as well. There are a number of expectations that we have for what each of these quantities will be sensitive to. They are listed in the following table.

Asym	East	West
$\widetilde{A}^{B}_{N,LR}$	0	$P_B^{T,\mathrm{vert}}$
$\widetilde{A}^{Y}_{N,LR}$	$P_Y^{T,\mathrm{vert}}$	0
$\widetilde{A}^{B}_{N,TB}$	0	$P_B^{T,\mathrm{horiz}}$
$\widetilde{A}^{Y}_{N,TB}$	$P_Y^{T,\mathrm{horiz}}$	0

where "0" means that the quantity should be exactly 0, unless there is a problem in the detector in some manner. (This is from the simple observation that in transverse spin asymmetries, the asymmetry is for $x_F > 0$ and not for $x_F < 0$).

Each of these ratios, $\widetilde{A}$ can be made into an analyzing power, A_N using the following formula

$$A_N = \frac{\widetilde{A_N} - 1}{\widetilde{A_N} + 1} \tag{20}$$

Similarly there are a number of ratios that are sensitive to double spin effects. The ratios that we calculate in this note are

$$\widetilde{A}_{LR}^{PP-PM} = \sqrt{\frac{(N_L^{++}+N_L^{--})(N_R^{+-}+N_R^{-+})}{(N_L^{+-}+N_L^{-+})(N_R^{++}+N_R^{--})}} \tag{21}$$

$$\widetilde{A}_{TB}^{PP-PM} = \sqrt{\frac{(N_T^{++}+N_T^{--})(N_B^{+-}+N_B^{-+})}{(N_T^{+-}+N_T^{-+})(N_B^{++}+N_B^{--})}} \tag{22}$$

Finally there are a few ratios that should be 1 because they are detector asymmetries and are used as a cross check to make sure everything is calculated and measured correctly. They are defined as

$$\widetilde{A}_{N,C}^{B} = \sqrt{\frac{(N_{C1}^{++}+N_{C1}^{+-})(N_{C2}^{-+}+N_{C2}^{--})}{(N_{C1}^{-+}+N_{C1}^{--})(N_{C2}^{++}+N_{C2}^{+-})}} \tag{23}$$

$$\widetilde{A}_{N,C}^{Y} = \sqrt{\frac{(N_{C1}^{++}+N_{C1}^{-+})(N_{C2}^{+-}+N_{C2}^{--})}{(N_{C1}^{+-}+N_{C1}^{--})(N_{C2}^{++}+N_{C2}^{-+})}} \tag{24}$$

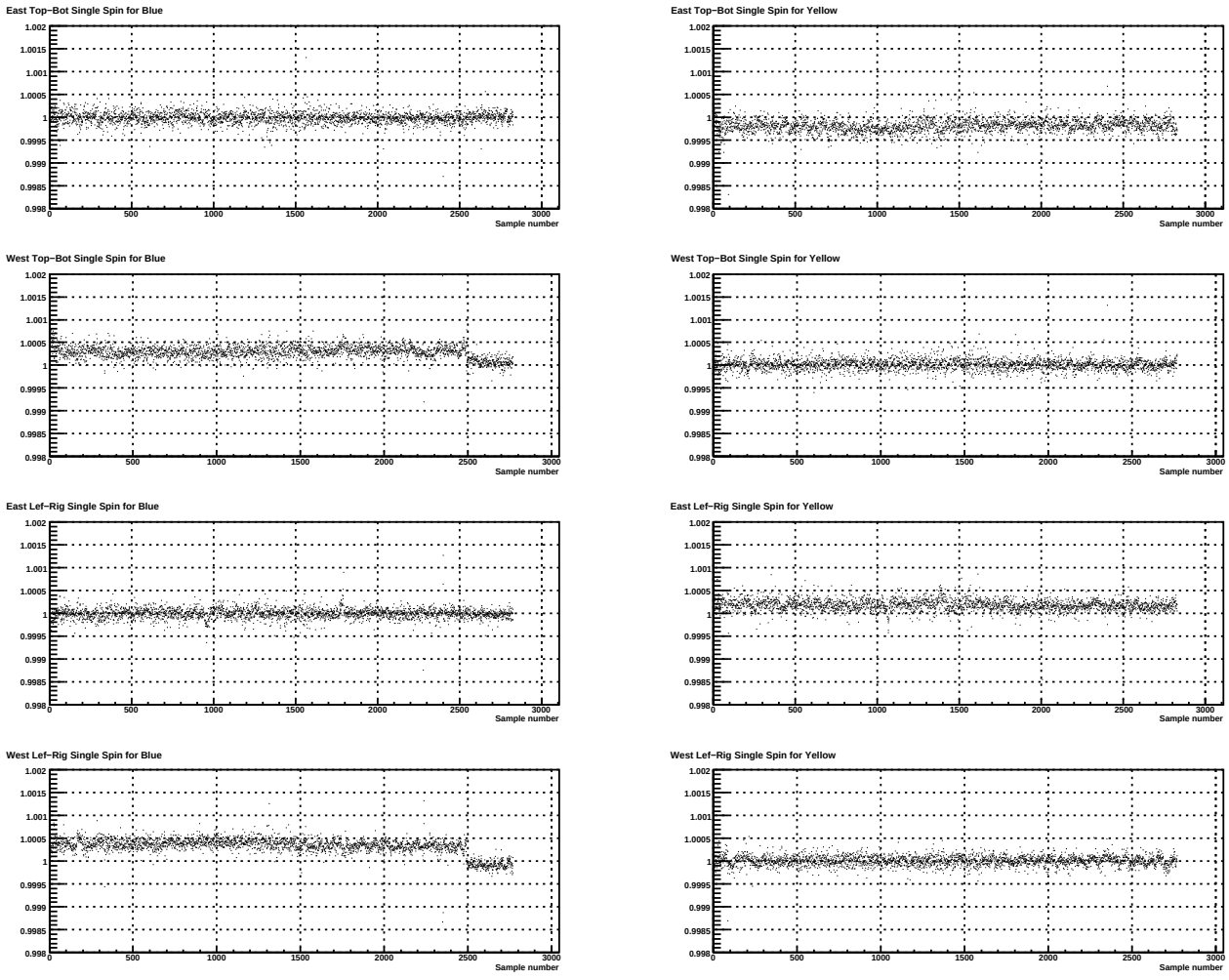

Figure 14: The 8 single spin asymmetries defined in equation blah versus filenumber (arb. count)

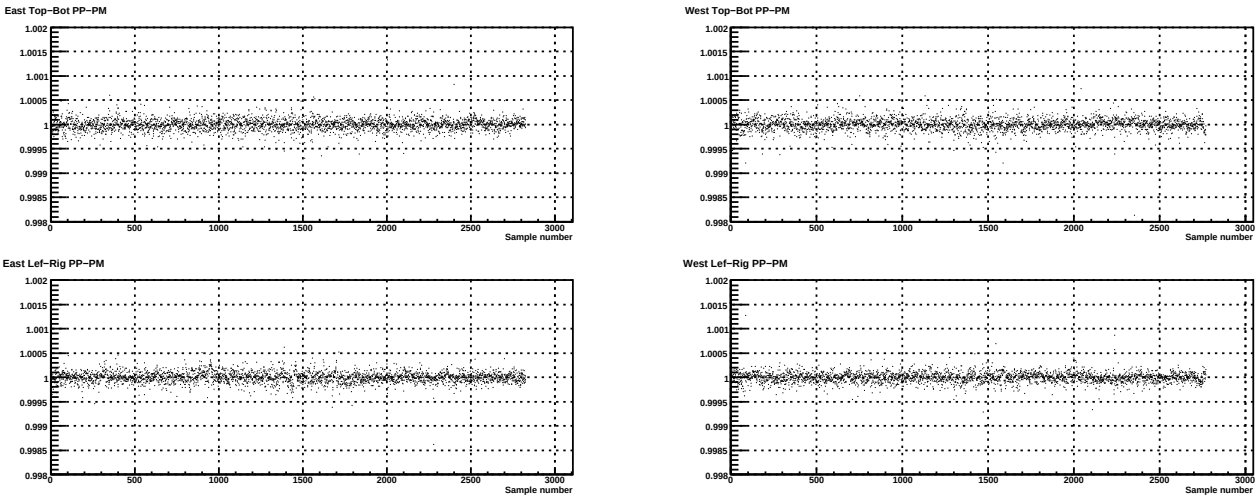

Figure 15: The 4 double spin asymmetries defined in equation blah versus filenumber (arb. count)

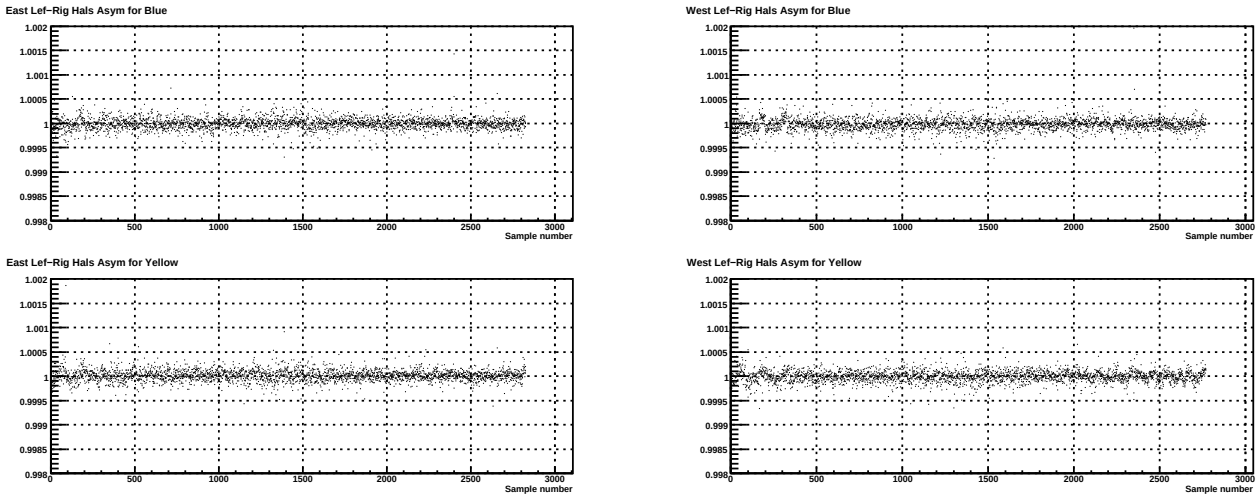

Figure 16: The 4 detector asymmetries defined in equation blah versus filenumber (arb. count)

5.1 Discussion of the Results from Boards 11 and 12

The results in figure blah, the single spin asymmetries, are the most interesting part form this section as they show the only spin dependence. The single spin asymmetries that are sensitive to the transverse beam spin component in either beam show non-unity values across all runs. You can also see the effect where the rotators were tuned for the blue beam (run # 10173050 $\simeq$ 2500 in the arb. units). This means that both beams had significant transverse spin components throughout the entire run9.

The asymmetries that are sensitive to double spin asymmetries or to detectors asymmetries are all 1 to well within the uncertainties and exhibit no clear systematic effects.

6 Systematic Studies of Relative Luminosity

6.1 Board 4 Studies

6.1.1 Comparison between boards 4 and 6

6.2 Spin Pattern Dependence

6.3 Rotator Tuning Effects

6.4 Rate Dependence Effects

6.5 A/M Summing Approach Studies

6.6 Corrected ZDCX/BBCX versus bunch crossing number

7 Evaluation of Possible Causes for Difference in Relative Luminosities

Several different possibilities have been evaluated and tested against the ZDC and BBC relative luminosity data. These will be presented in the following sections. None has shown good agreement with the data. In addition, a number of differences between the blue and yellow beams during run9 (and also run6) are noted. It is not clear if or how many of these are related to the difference in calculated relative luminosities. However, they are noted here in case someone else can figure out a mechanism to produce the observed results from this information.

7.1 A_{LL} in the BBC and/or ZDC

It was suggested that the differences in calculated relative luminosities might be caused by a two-spin A_{LL} for the processes observed by one or both luminosity monitors. Assuming this is the only cause of the differences, then the number of counts observed in the ZDC for the 4 spin states would be

$$N^{++}_{\rm ZDC} = N_{0,\rm ZDC} L^{++} d\Omega_{\rm ZDC} \left(1 + P^+_B P^+_Y A_{LL,\rm ZDC}\right) \quad (25)$$
$$N^{+-}_{\rm ZDC} = N_{0,\rm ZDC} L^{+-} d\Omega_{\rm ZDC} \left(1 - P^+_B P^-_Y A_{LL,\rm ZDC}\right) \quad (26)$$
$$N^{-+}_{\rm ZDC} = N_{0,\rm ZDC} L^{-+} d\Omega_{\rm ZDC} \left(1 - P^-_B P^+_Y A_{LL,\rm ZDC}\right) \quad (27)$$
$$N^{--}_{\rm ZDC} = N_{0,\rm ZDC} L^{--} d\Omega_{\rm ZDC} \left(1 + P^-_B P^-_Y A_{LL,\rm ZDC}\right) \quad (28)$$

The true luminosities are L^{++}, etc, the solid angle times the efficiency are given by $d\Omega$, the blue and yellow beam polarization magnitudes are $P^+_B = P^-_B$ and $P^+_Y = P^-_Y$ (under these assumptions), and $N_{0,\rm ZDC}$ is a normalization constant. Then

$$\frac{N^{++}_{\rm ZDC}}{N^{--}_{\rm ZDC}} = \frac{L^{++}}{L^{--}} \qquad \frac{N^{+-}_{\rm ZDC}}{N^{-+}_{\rm ZDC}} = \frac{L^{+-}}{L^{-+}} \quad (29)$$

and similarly for the BBC. As a result , it would be expected that

$$\epsilon(R_4) = 0 \qquad \text{and} \qquad \epsilon(R_5/R_6) = 0 \quad (30)$$

However the observed results (from table blah) strongly violate these conditions. Hence it is concluded that an A_{LL} for processes in the BBC and/or the ZDC is not the sole cause of the difference in relative luminosities.

7.2 A_L in the BBC and/or ZDC

The case of a parity violating asymmetry in one or both luminosity monitors is very similar to the previous one. The equations for the number of counts become

$$\begin{aligned}
N^{++}_{\rm ZDC} &= N_{0,\rm ZDC} L^{++} d\Omega_{\rm ZDC} \left(1 + P^+_B A_{L,\rm ZDC} + P^+_Y A_{L,\rm ZDC}\right) && (31)\\
N^{+-}_{\rm ZDC} &= N_{0,\rm ZDC} L^{+-} d\Omega_{\rm ZDC} \left(1 + P^+_B A_{L,\rm ZDC} - P^-_Y A_{L,\rm ZDC}\right) && (32)\\
N^{-+}_{\rm ZDC} &= N_{0,\rm ZDC} L^{-+} d\Omega_{\rm ZDC} \left(1 - P^-_B A_{L,\rm ZDC} + P^+_Y A_{L,\rm ZDC}\right) && (33)\\
N^{--}_{\rm ZDC} &= N_{0,\rm ZDC} L^{--} d\Omega_{\rm ZDC} \left(1 - P^-_B A_{L,\rm ZDC} - P^-_Y A_{L,\rm ZDC}\right) && (34)
\end{aligned}$$

Again, $P^+_B = P^-_B = P_B$ and $P^+_Y = P^-_Y = P_Y$ so if $A_{L,\rm BBC} = 0$, then we have

$$\epsilon(R_4) = (P_Y + P_B) A_{L,\rm ZDC} \qquad \text{and} \qquad \epsilon(R_5/R_6) = (P_Y - P_B) A_{L,\rm ZDC} = 0 \tag{35}$$

The expression for $\epsilon(R_5/R_6)$ is expected to be near zero because usually $P_B \simeq P_Y$, but the observed value differs significantly from zero (-0.00135 ± 0.0004). Thus it is concluded that an A_L for the ZDC cannot be the sole cause of the difference in relative luminosities. THe same argument obviously holds for an A_L in the BBC. If there are parity violating A_L's for both monitors, then

$$\begin{aligned}
\epsilon(R_4) &= (P_Y + P_B)(A_{L,\rm ZDC} - A_{L,\rm BBC}) + \text{h.o.t.} && (36)\\
\epsilon(R_5/R_6) &= (P_Y - P_B)(A_{L,\rm ZDC} - A_{L,\rm BBC}) + \text{h.o.t.} && (37)
\end{aligned}$$

where the higher order terms (h.o.t.) involve products of $P_Y P_B A_{L,\rm ZDC} A_{L,\rm BBC}$ and thus are expected to be negligible. Again, $\epsilon(R_5/R_6)$ should be very small.

7.3 Combined A_L and A_{LL} Effects

The expression relating the observed counts to both an A_L and an A_{LL} are straightforward extensions of those give in sections blah and blah. For example

$$\begin{aligned}
N^{+-}_{\rm ZDC} &= N_{0,\rm ZDC} L^{+-} d\Omega_{\rm ZDC} \left(1 + P^+_B A_{L,\rm ZDC} - P^-_Y A_{L,\rm ZDC} - P^+_B P^-_Y A_{LL,\rm ZDC}\right) && (38)\\
&= N_{0,\rm ZDC} L^{+-} d\Omega_{\rm ZDC} \left(1 + [P_B - P_Y] A_{L,\rm ZDC} - P_B P_Y A_{LL,\rm ZDC}\right) && (39)
\end{aligned}$$

and the other spin configuration follow from analogous math. Then as before

$$\begin{aligned}
\epsilon(R_4) &= (P_Y + P_B)(A_{L,\rm ZDC} - A_{L,\rm BBC}) + \text{h.o.t} && (40)\\
\epsilon(R_5/R_6) &= (P_Y - P_B)(A_{L,\rm ZDC} - A_{L,\rm BBC}) + \text{h.o.t} && (41)
\end{aligned}$$

where now the higher order terms contain products such as $P_Y A_{L,\rm ZDC} P_B P_Y A_{LL,\rm BBC}$ as well as $P_B A_{L,\rm ZDC} P_Y A_{L,\rm BBC}$. In any case, $\epsilon(R_5/R_6)$ should be very small and experimentally it is not!

7.4 Effects of Transverse Beam Spin Components

A difference in relative luminosities could arise due to transverse beam spin components, an A_N for the physics process(es) detected and an offset of the (projected) beam at the luminosity monitor. The discussion will be focused on effects in the ZDC, since A_N is observed to be much larger than for the BBCs, though in principle such effects could also be present for the BBCs.

The luminosity monitor will be assumed to be the coincidence of signals from east and west ZDCs (or BBCs). Offset of the beam projected to the ZDCs will be presumed to occur in both beams, and initially the transverse spin components will be assumed to be up/down. Defining $d\Omega_{LR}$ to be the ZDC solid angle times efficiency times cross section for the blue beam to be left of the projected beam center on the west and the yellow beam to be right of the center on the east, then

$$\begin{aligned} N^{++} = N_{0,\mathrm{ZDC}} L^{++} [&(d\Omega_{LL} + d\Omega_{LR} + d\Omega_{RL} + d\Omega_{RR}) \\ &+ (d\Omega_{LL} + d\Omega_{LR}) P^{+}_{B,N} A_{N,\mathrm{ZDC}} - (d\Omega_{RL} + d\Omega_{RR}) P^{+}_{B,N} A_{\mathrm{ZDC}} \\ &+ (d\Omega_{LL} + d\Omega_{RL}) P^{+}_{Y,N} A_{N,\mathrm{ZDC}} - (d\Omega_{LR} + d\Omega_{RR}) P^{+}_{Y,N} A_{N,\mathrm{ZDC}}] \end{aligned} \tag{42}$$

$$\begin{aligned} N^{+-} = N_{0,\mathrm{ZDC}} L^{+-} [&(d\Omega_{LL} + d\Omega_{LR} + d\Omega_{RL} + d\Omega_{RR}) \\ &+ (d\Omega_{LL} + d\Omega_{LR}) P^{+}_{B,N} A_{N,\mathrm{ZDC}} - (d\Omega_{RL} + d\Omega_{RR}) P^{+}_{B,N} A_{\mathrm{ZDC}} \\ &- (d\Omega_{LL} + d\Omega_{RL}) P^{+}_{Y,N} A_{N,\mathrm{ZDC}} + (d\Omega_{LR} + d\Omega_{RR}) P^{+}_{Y,N} A_{N,\mathrm{ZDC}}] \end{aligned} \tag{43}$$

$$\begin{aligned} N^{-+} = N_{0,\mathrm{ZDC}} L^{-+} [&(d\Omega_{LL} + d\Omega_{LR} + d\Omega_{RL} + d\Omega_{RR}) \\ &- (d\Omega_{LL} + d\Omega_{LR}) P^{+}_{B,N} A_{N,\mathrm{ZDC}} + (d\Omega_{RL} + d\Omega_{RR}) P^{+}_{B,N} A_{\mathrm{ZDC}} \\ &+ (d\Omega_{LL} + d\Omega_{RL}) P^{+}_{Y,N} A_{N,\mathrm{ZDC}} - (d\Omega_{LR} + d\Omega_{RR}) P^{+}_{Y,N} A_{N,\mathrm{ZDC}}] \end{aligned} \tag{44}$$

$$\begin{aligned} N^{--} = N_{0,\mathrm{ZDC}} L^{--} [&(d\Omega_{LL} + d\Omega_{LR} + d\Omega_{RL} + d\Omega_{RR}) \\ &- (d\Omega_{LL} + d\Omega_{LR}) P^{+}_{B,N} A_{N,\mathrm{ZDC}} + (d\Omega_{RL} + d\Omega_{RR}) P^{+}_{B,N} A_{\mathrm{ZDC}} \\ &- (d\Omega_{LL} + d\Omega_{RL}) P^{+}_{Y,N} A_{N,\mathrm{ZDC}} + (d\Omega_{LR} + d\Omega_{RR}) P^{+}_{Y,N} A_{N,\mathrm{ZDC}}] \end{aligned} \tag{45}$$

And with these quantities we have

$$\epsilon(R_4) = (\epsilon_{\Omega W} P_{B,N} + \epsilon_{\Omega E} P_{Y,N}) A_{N,\mathrm{ZDC}} + \mathrm{h.o.t.} \tag{46}$$

$$\epsilon(R_5) = \epsilon_{\Omega E} P_{Y,N} A_{N,\mathrm{ZDC}} + \mathrm{h.o.t.} \tag{47}$$

$$\epsilon(R_6) = \epsilon_{\Omega W} P_{B,N} A_{N,\mathrm{ZDC}} + \mathrm{h.o.t.} \tag{48}$$

where we have

$$\epsilon_{\Omega W} = \frac{d\Omega_{LL} + d\Omega_{LR} - d\Omega_{RL} - d\Omega_{RR}}{d\Omega_{LL} + d\Omega_{LR} + d\Omega_{RL} + d\Omega_{RR}} \tag{49}$$

$$\epsilon_{\Omega W} = \frac{d\Omega_{LL} + d\Omega_{RL} - d\Omega_{LR} - d\Omega_{RR}}{d\Omega_{LL} + d\Omega_{LR} + d\Omega_{RL} + d\Omega_{RR}} \tag{50}$$

In particular you have

$$\epsilon(R_4) - \epsilon(R_5) - \epsilon(R_6) \simeq 0 \tag{51}$$

Although the transverse spin directions may not have been up/down, similar expression can be derived. The difference is that instead of the "solid angle asymmetries" ($\epsilon_{\Omega E}$ and $\epsilon_{\Omega W}$) corresponding

to left-right asymmetries, they would then be along the direction perpendicular to the transverse spin (and the beam)

Comparing equation **??** with the data in section blah, indicates that transverse spin components plus the ZDC A_N plus beam offsets at the ZDCs is not the sole cause of the observed differences in relative luminosities.

7.5 Combined Transverse Spin Effects and A_{LL}

Another possibility is that a pair of effects - A_{LL} in the ZDCs and/or BBCs (subsection blah) plus the transverse spin component effects of subsection blah are responsible for the differences in relative luminosities. Then, to equations blah, for the counts, will be added terms of the form

$$\pm N_{0,\mathrm{ZDC}} L d\Omega_{\mathrm{ZDC}} P^{\pm}_{BL} P^{\pm}_{YL} A_{LL,\mathrm{ZDC}} \tag{52}$$

or similarly for the BBC, where

$$d\Omega_{\mathrm{ZDC}} = d\Omega_{LL} + d\Omega_{LR} + d\Omega_{RL} + d\Omega_{RR}. \tag{53}$$

The P_{BL} and P_{YL} are the blue and yellow longitudinal polarization magnitudes for the particular spin states. See equations blah in subsection blah for the pattern of the added terms. Solving these equations leads to

$$\begin{aligned}
\epsilon(R_4) =& (\epsilon_{\Omega W} P_{BN} + \epsilon_{\Omega E}) P_{Y,N} A_{N,\mathrm{ZDC}} \\
&+ P_{B,L} P_{Y,L} (A_{LL,\mathrm{ZDC}} - A_{LL,\mathrm{BBC}})(\epsilon_{PB} + \epsilon_{PY}) + \text{h.o.t.} && (54)\\
\epsilon(R_5) =& \epsilon_{\Omega E} P_{Y,N} A_{N,\mathrm{ZDC}} \\
&- P_{B,L} P_{Y,L} (A_{LL,\mathrm{ZDC}} - A_{LL,\mathrm{BBC}})(1 - \epsilon_{PB}) + \text{h.o.t.} && (55)\\
\epsilon(R_6) =& \epsilon_{\Omega W} P_{B,N} A_{N,\mathrm{ZDC}} \\
&- P_{B,L} P_{Y,L} (A_{LL,\mathrm{ZDC}} - A_{LL,\mathrm{BBC}})(1 - \epsilon_{PY}) + \text{h.o.t.} && (56)
\end{aligned}$$

where

$$\epsilon_{PB} = \frac{P^{+}_{B,L} - P^{-}_{B,L}}{P^{+}_{B,L} + P^{-}_{B,L}} \qquad \text{and} \qquad \epsilon_{P,Y} = \frac{P^{+}_{Y,L} - P^{-}_{Y,L}}{P^{+}_{Y,L} + P^{-}_{Y,L}}. \tag{57}$$

Then, in particular

$$\epsilon(R_4) - \epsilon(R_5) - \epsilon(R_6) = 2 P_{B,L} P_{Y,L} (A_{LL,\mathrm{ZDC}} - A_{LL,\mathrm{BBC}}) + \text{h.o.t.} \tag{58}$$

Thus the transverse spin effects and difference in longitudinal beam polarizations (ϵ_{PB} and ϵ_{PY}) all cancel to leading order in this expression. Evaluating this equation for all runs or for only those after the spin rotator adjustment gives 0.00108 and 0.00059, respectively. This is not very good agreement, and the beam polarizations did not drop significantly after the beam rotator changes (include table for individual spin states??)

Note that with $P_{B,L} \simeq P_{Y,L} \simeq 0.5$, then

$$(A_{LL,\mathrm{ZDC}} - A_{LL,\mathrm{BBC}}) \simeq 0.0012 - 0.0022. \tag{59}$$

7.6 Beam "Migration" Into Following Bunches

One feature of the measurements that has not been addressed by any of the possible explanations so far is the difference in results as a function of spin pattern. One possible mechanism would be beam "migrating" from one bunch to the following bunch, perhaps due to very small angle Coulomb scattering at an interaction region or scattering off beam pipe walls when the beam size is large in quadrupoles. These effects could be spin dependent. Also, the blue and yellow beams could differ because the blue beam generally had a shorter lifetime (and large emittance).

A simple model of this possible explanation was made. It was assumed that all beam bunches had the same intensity on average. The migration fractions were taken to be a, b for the $+$, $-$ bunches in the blue beam and c, d for the $+$, $-$ bunches in the yellow beam. Although the first bunch after an abort gap would receive no additional beam, whereas other bunches would, this effect was ignored.

The following table gives the blue spin, blue intensity (corrected for loss to the following bunch and gains from the previous bunch), yellow spin, yellow intensity, the (BY) spins, and the bunch crossing luminosity for one cycles (8 bunch crossings) for the spin pattern "5". Spin pattern "9" is identical except offset by 4. From the values, sums for the luminosity of $++$, $+-$, $-+$ and $--$ can be obtained and the ratio computed for these spin patterns and they are shown in the following table

blue spin	blue intensity	yellow spin	yellow intensity	BY spin	bunch crossing lumi
$+$	$N(1-a+a)$	$+$	$N(1-c+d)$	$++$	$L(1-c+d)$
$-$	$N(1-b+a)$	$+$	$N(1-c+c)$	$-+$	$L(1+a-b)$
$+$	$N(1-a+b)$	$-$	$N(1-d+c)$	$+-$	$L(1-a+b+c-d)$
$-$	$N(1-b+a)$	$-$	$N(1-d+d)$	$--$	$L(1+a-b)$
$-$	$N(1-b+b)$	$+$	$N(1-c+d)$	$-+$	$L(1-c+d)$
$+$	$N(1-a+b)$	$+$	$N(1-c+c)$	$++$	$L(1-a+b)$
$-$	$N(1-b+a)$	$-$	$N(1-d+c)$	$--$	$L(1+a-b+c-d)$
$+$	$N(1-a+b)$	$-$	$N(1-d+d)$	$+-$	$L(1-a+b)$

With this we can calculate

$$\epsilon(R_4) \simeq -\frac{3}{2}(a-b)-(c-d) \tag{60}$$
$$\epsilon(R_5) \simeq -\frac{1}{2}(a-b)-(c-d) \tag{61}$$
$$\epsilon(R_6) \simeq -2(a-b) \tag{62}$$
$$\tag{63}$$

and similarly for the other two spin patterns, "6" and "10."

$$\epsilon(R_4) \simeq -\frac{3}{2}(a-b)-(c-d) \tag{64}$$
$$\epsilon(R_5) \simeq +\frac{1}{2}(a-b)-(c-d) \tag{65}$$
$$\epsilon(R_6) \simeq -(a-b) \tag{66}$$
$$\tag{67}$$

The data show $\epsilon(R_6)$ very small and $\epsilon(R_4) \neq \epsilon(R_5)$, thus, this explanation is not the sole cause of the difference in relative luminosity.

7.7 Possible Related Observations

The previous subsections attempted to explain the differences in relative luminosity based on particular assumptions, for example, an A_{LL} in the BBCs and/or the ZDCs. None of these attempts were very successful. A number of possible mechanisms are given here. In these cases, the mechanism alone will not explain the results, but perhaps combined with another mechanism here or in a previous subsection is the true cause of the differences.

1) The blue beam was always injected into RHIC first, and generally had a shorted lifetime and larger phase space or emittance than the yellow beam.

2) The beams interacted continuously with the hydrogen gas jet target. Bending the DX magnet after this target may have led to preferential loss of scattered beam for one spin states compared to the other (due to the nonzero A_N for scattering on the hydrogen jet). This could have differed for the two beams because of difference in phase space or emittance (see item above).

3) For transverse beam operation everywhere in RHIC, the blue beam makes a left bend after the STAR interaction region and the yellow beam makes a right bend. As in item 2 above, this may have led to larger losses of beam scattered from residual gas for one spin state compared to the other. Because of the Siberian Snakes between the 2 and 4 o'clock and 8 and 10 o'clock intersection regions, which flipped the spin direction of the beam from up to down and vice versa, the only other equivalent location to STAR would be at 10 o'clock. The other 3 intersection regions would all be opposite. For the data studied here, STAR ran with longitudinal beams (what about PHENIX?), but there was transverse beam polarization at all other intersections regions.

4) Various people have reported "afterpulsing" or "ringing" of photomultipler signals from both the BBC and ZDC counters. These could cause undesired accidental coincidences with following bunches. Evidence of the afterpulsing is perhaps observable in figs blah. Other effects, such as pulse widths of logic signals or "tails" on photomultiplier signals may also contribute to accidentals in following bunches. This afterpulsing may affect multiple bunches after the triggering bunch, whereas the calculation in subsection 7.6 assumed an effect on only the bunch immediately following.

5) The acceptance of events along the beam for the ZDCs and BBCs is expected to be difference because of the considerable difference in distance of these detectors from the center of the intersection region (18m vs 3.7?m). This would have to couple to longer or shorted bunches correlated with spin sate or to polarization direction change from front to middle to back of bunches. Mei Bai said the latter effect was conceivable.

6) The first bunch after or the last bunch before an abort gap could conceivably have different emittance. or phase space while filling RHIC. However, the spin of these bunches varies with the spin pattern, and this effect along would be expected to average to zero when summing over all four spin patterns. It would need to be coupled with some other effect, perhaps beam "migration" of subsection 7.6 or photomultiplier afterpulsing, in order to produce the observed difference in relative luminosities.

7) The blue beam spin patterns was always

$$+-+--+-++-+--+-++-+--+-+...$$

while the yellow spin pattern was always

$$++--++--++--++--++--++--...$$

during run9. Then, in the blue beam, a + bunch was following by a − bunch almost three times more often than by a + bunch. SImilarly, a − bunch was following by a + bunch about three times more often than by a − bunch. For the yellow beam, the probabilities were all approximately equal. While this was studied with beam migration effects in subsection 7.6, perhaps too many simplifying assumptions were made or other effects were also present.

8) There was one bunch (# 20, counting from 0 after the abort gap) in each beam that is perturbed or "kicked" to monitor the beam tunes. This bunch at times had lower intensity and possible larger phase space or emittance than the other bunches (see Ref?). In addition there are nice missing bunches in each abort gap, while the spin pattern repeats every 8 bunches. Thus, the number of bunch crossing differed for the various spin combinations, assuming bunch #20 was omitted from those used :

Spin Pattern	++	+−	−+	−−	#20
"5"	26	24	24	26	−+
"6"	24	26	26	24	−−
"9"	24	26	26	24	++
"10"	26	24	24	26	+−

The differences in number of the four spin configurations could affect the relative luminosities perhaps if coupled with beam migrations or afterpulsing of photomultipliers. Note that the calculation in subsection 7.6 ignored this effect.

9) The beam during longitudinal runs have a large horizontal transverse spin component between the DX magnets and the nearby ZDCs all the way to the spin rotators. This component would have changed significantly before and after the rotator tuning in run9. It is hypothesized that the sizable changes for the relative luminosity asymmetries separated by spin state before and after the rotator adjustment are in some way related to the change in this spin component. Perhaps there is scattering from the walls of the beam pipe producing more particles up or down, depending on the sign of the pin. It is to be noted that the beam size is quite large in the low-β quadupoles between the DX magnets and the spin rotators. In addition, an asymmetry in the ZDC up-down acceptance would be required.

10) It is possible that the + and − bunches in a beam had slightly different properties, and thus may have differed for the blue and yellow beams. Such differences might have been that the + bunches were slightly fatter or longer or were displaces to the left or displaced longitudinally forward on average compared to the − bunches. This could be studies by evaluating bunch shapes from many fills similar to that performed in the ref blah for a couple fills. The polarization profile,

both longitudinally and transversely, could also conceivably differ on average. With the transverse profile could be studied for the few fills where polarizations profile measurements were performed, no longitudinal profile has been obtained yet, and of course these profiles are for the transverse spin components only. If such differences were observed, the origin may not be obvious - from polarized ion source to any of the several accelerators including RHIC.

11) It has been pointed out that the ZDC spacing ($2 \times 18\text{m} \rightarrow 120$ sec) is nearly the same as the bunch spacing (~ 108 ns). Therefore, secondaries from beam-gas interactions or some beam particles interacting with the beam pipe walls would arrive at the ZDCs close to the correct time for particles from beam-beam interactions at the center of the intersection region. One would expect these to be accounted for with accidentals corrections, but...

12) The planes of the AGS and RHIC accelerators are at different elevations. A horizontal bend is made between the two vertical bends to compensate for the elevation difference in the AtR (AGS to RHIC) transfer lines. This (plus ___) results in the ___ beam being nearly purely vertically polarized, but the ____ beam having a sizable ___ component, upon injection into RHIC. (IS this correct? What are the missing pieces above?)

A Introduction to the Scaler Boards

The scaler boards are simple counters that 'scale' whatever the input signal is that they are supplied with. You can think of them as possessing a number of independent integers that each time the board receives a positive signal (binary 1, and 0 for no signal) the integer associated with that signal increases by 1 count.

In STAR, the scaler boards typically scale quantities associated with the fast, high rate detectors like the BBCs, ZDCs, and VPDs. The quantities they scale are usually trigger-like quantities such that a clear binary signal can be formed by setting a threshold of some sort on the detector signals. The definitions of the signals and their precise mappings to the various scaler boards can be found in appendices blah and blah.

In run9, all the scaler boards used are 24-bit scaler boards. This refers to the 24 input signals that are routed into the boards. The STAR scaler boards are designed to scale all 2^{24} possible combinations of the 24 input signals. That is to say that each board has 2^{24} independent counters that add 1 to their tally each time the 24 input signals correspond to the pattern of a particular counter.

Each counting integer is a 40-bit integer so that it can count from 0 to $2^{40} - 1 \simeq 10^{12}$ which means that any counter can run for 10^5 seconds (~ 3 hours) before it could possibly saturate its counter bits.

Now, cleverly, STAR sets 7 of the input signals to be associated with the bunch crossing number so that each bunch crossing has independent counts of the other 2^{17} possible combinations of the input bits. It is in this way that STAR manages to scale all of our fast detectors bunch crossing by bunch crossing to calculate the relative luminosity.

B Scaler Board Mappings for Run 9 pp 200

This section details the mappings of inputs and algorithms to the bits on the scaler boards 4, 6, 11 and 12.

C Scaler Board Input Algorithms and Definitions

C.1 vt201